

Copyright © 2009. Reprinted from APPLIED PHYSICS LETTERS. 95, 153304.2009. Such permission of the American Institute of Physics does not in any way imply the American Institute of Physics endorsement of any of Institute of Microelectronics' products or services. Internal or personal use of this material is permitted. However, permission to reprint/republish this material for advertising or promotional purposes or for creating new collective works for resale or redistribution must be obtained from the American Institute of Physics by writing to Rights@aip.org.

An inverted organic solar cell with an ultrathin Ca electron-transporting layer and MoO₃ hole-transporting layer

D. W. Zhao,^{1,2} P. Liu,¹ X. W. Sun,^{1,a)} S. T. Tan,² L. Ke,³ and A. K. K. Kyaw¹

¹*School of Electrical and Electronic Engineering, Nanyang Technological University, Nanyang Avenue, Singapore 639798, Singapore*

²*Institute of Microelectronics, A*STAR (Agency for Science, Technology and Research), 11 Science Park Road, Science Park II, Singapore 117685, Singapore*

³*Institute of Materials Research and Engineering, A*STAR (Agency for Science, Technology and Research), 3 Research Link, Singapore 117602, Singapore*

(Received 30 July 2009; accepted 28 September 2009; published online 16 October 2009)

An inverted organic solar cell based on poly(3-hexylthiophene) (P3HT) and 1-(3-methoxycarbonyl)-propyl-1-phenyl-(6,6)C₆₁ (PCBM) was fabricated with an ultrathin Ca electron-transporting layer and MoO₃ hole-transporting layer. The 1 nm Ca on indium tin oxide (ITO) electrode modifies the work function of ITO suitable for electron extraction. An appropriate thickness of MoO₃ hole extraction layer is also essential to effectively prevent exciton quenching at the Ag anode, yet not introduce much voltage loss and series resistance. The optical field distribution across the active layer was also simulated to discuss the effect of MoO₃ thickness on the photocurrent. The maximum power conversion efficiency obtained was 3.55% under simulated 100 mW/cm² (AM 1.5G) solar irradiation. © 2009 American Institute of Physics.

[doi:10.1063/1.3250176]

Organic solar cells (OSCs) have attracted much attention in the past few years.¹⁻⁵ Most OSCs employ a conductive poly(3,4-ethylenedioxythiophene): poly(styrene-sulfonate) (PEDOT:PSS) layer as the hole-transporting layer. PEDOT:PSS is aqueous and naturally acidic, which would cause interface instability.^{3,6} Moreover, a low work function (LWF) metal prone to oxidation/degradation has to be used on top of the OSC, which leads to device instability as well.⁶ To overcome the instability issue associated with the normal structured OSC, one feasible approach is to construct an inverted device, where indium tin oxide (ITO) serves as the cathode and a high work function metal as the anode. However, ITO cannot serve as cathode directly. It requires interfacial modification with functional buffer layers such as TiO_x (Ref. 7) and ZnO (Refs. 8 and 9) for hole blocking, and Cs₂CO₃ (Refs. 10 and 11) for lowering the work function of ITO for efficient electron extraction. As an alternative, modifying ITO by a LWF metal would be an effective approach to lower the work function of ITO. However, there is no such report thus far.

On the other hand, for the anode side, an interfacial buffer layer, such as PEDOT:PSS,¹² V₂O₅,³ and WO₃,¹³ is inserted between the active layer and metal to improve the hole transport and extraction. Except for the role of the hole transport and extraction, such an anode buffer layer also acts as an optical spacer,¹⁴ adjusting the effective optical field distribution in the entire device.

In this letter, we shall present an inverted OSC with a Ca electron-transporting layer and MoO₃ hole-transporting layer. Optical field distribution was simulated to show the effect of MoO₃ thickness on the optical field distribution across the active layer.

All cells were fabricated on ITO coated glass substrates with a sheet resistance of 20 Ω/□. A Ca layer was first thermally evaporated under a base vacuum of 9.0 × 10⁻⁵ Pa. Then, a blend solution made of poly(3-hexylthiophene) (P3HT) (Rieke Metals, Inc.) and 1-(3-methoxycarbonyl)-propyl-1-phenyl-(6,6)C₆₁ (PCBM) (American Dye Sources Inc.) with a weight ratio of 1:0.8 in chlorobenzene (30 mg/ml) was spin coated onto Ca coated ITO substrate to form the active layer in a glove box filled with N₂ (H₂O < 0.1 ppm and O₂ < 0.1 ppm). Subsequently, MoO₃ and Ag were evaporated sequentially (9.0 × 10⁻⁵ Pa), followed by postannealing at 160 °C for 10 min. Finally, the cells with an active area of 0.1 cm² were encapsulated before taking out from the glove box. The current-voltage (*I*-*V*) characteristics were measured with a Keithley 2400 sourcemeter under simulated 100 mW/cm² (AM 1.5G) irradiation from a solar simulator (Solar Light Co. Inc.). The transmittance spectra of the samples were recorded using UV-visible-near IR scanning spectrophotometer (UV-3101PC). The film thickness was measured with a surface profiler (Tencor P15). The incident photon-to-electron conversion efficiencies (IPCEs), i.e., spectral responses, were measured using a 200 W xenon lamp light source with a motorized monochromator (Oriel). The device structure is shown in the inset of Fig. 1(a). The inverted cells in this study have a structure of ITO/Ca/P3HT:PCBM(85 nm)/MoO₃/Ag(100 nm) with different thicknesses of Ca and MoO₃.

Figure 1(a) shows the transmittance spectra of Ca/P3HT:PCBM (85 nm) films (with ITO/glass substrate absorption extracted for all curves) with different Ca thickness. In order to avoid the oxidization of Ca when measuring the transmittance spectra, we overcoated Ca by an 85 nm P3HT:PCBM layer. With the increase of Ca thickness, the transmittance of the film does not change much in the absorption range of active layer (from 400 to 650 nm), indicat-

^{a)}Author to whom correspondence should be addressed. Electronic mail: exwsun@ntu.edu.sg.

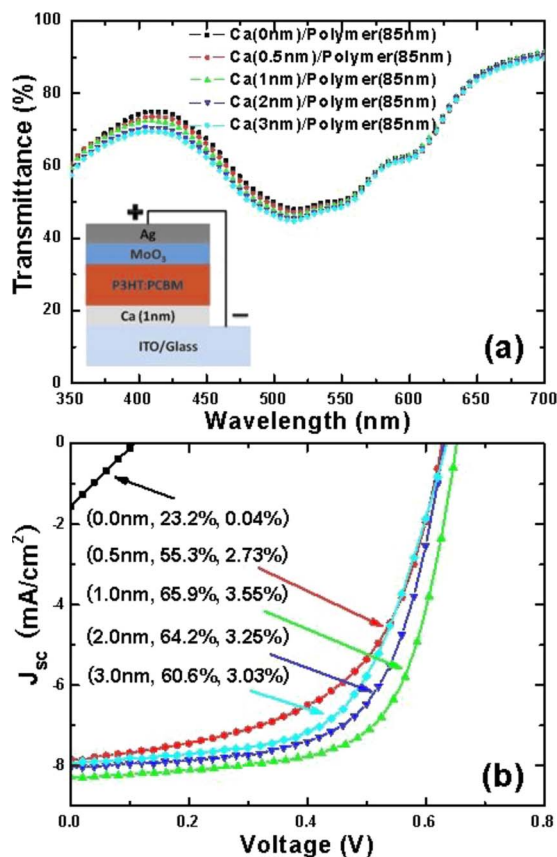


FIG. 1. (Color online) (a) The transmittance spectra of the films Ca(x nm)/P3HT:PCBM(85 nm) with $x=0, 0.5, 1, 2,$ and 3 nm. The inset shows the device structure of inverted OSC. (b) The J - V characteristics of inverted cells with 3 nm MoO₃ and different thicknesses of Ca under 100 mW/cm² illumination. The corresponding Ca thickness, FF, and PCE are shown in the format of (Ca thickness, FF, PCE).

ing that such an ultrathin Ca layer has a high transparency. The J - V characteristics of these inverted OSCs with 3 nm MoO₃ and different thicknesses of Ca under 100 mW/cm² are shown in Fig. 1(b). Without Ca, the cell is a hole-only device, exhibiting nearly no photovoltaic effect. The efficiency increases significantly when Ca is inserted. The short-circuit current density (J_{sc}) and fill factor (FF) increase first and then decrease as the Ca thickness increases. As a result, the optimal thickness of Ca layer is 1 nm, and its corresponding PCE reaches 3.55% . Similar to Cs₂CO₃ in inverted OSCs,³ Ca (~ 2.9 eV) first lowers the work function of ITO (~ 4.8 eV). The obtained open-circuit voltage (V_{oc}) approaches ~ 0.60 V for the cells with Ca layer. This demonstrates that the work function of Ca is pinned to the Fermi level of PCBM via the surface states. As a result, an Ohmic contact is favored between Ca and PCBM.^{15,16} Meanwhile, in contrast, a rectifying contact between Ca and P3HT will be formed,^{15,16} which will block the hole collection on the ITO side. Hence, ITO covered with Ca acts well as a cathode for electron collection. It is worth mentioning that the Ca layer was not oxidized (at least not fully), which was indirectly verified by a poorly performed control device with Ca being replaced by CaO (oxidizing Ca by dry air).

Figure 2(a) shows the J - V characteristics of various OSCs with 1 nm Ca and different MoO₃ thicknesses under 100 mW/cm². Obviously, in the absence or for a very thin layer of MoO₃ (0 or 1 nm), the J_{sc} and FF are close

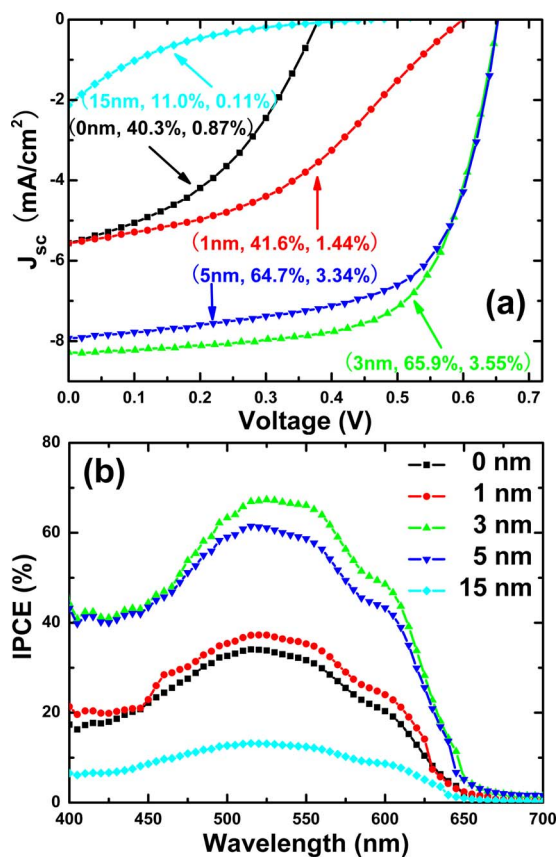


FIG. 2. (Color online) (a) The J - V characteristics of inverted cells with 1 nm Ca and different thicknesses of MoO₃ under 100 mW/cm² illumination. The corresponding MoO₃ thickness, FF, and PCE are shown in the format of (MoO₃ thickness, FF, PCE). (b) IPCEs of inverted cells with different thicknesses of MoO₃ layer.

except for a large difference in V_{oc} . For the cell with 3 nm MoO₃, the PCE remarkably increases to 3.55% with $J_{sc}=8.28$ mA/cm², $V_{oc}=0.65$ V, and FF= 65.9% . As the thickness of MoO₃ layer increases to 5 nm, the PCE slightly reduces to 3.34% with $J_{sc}=7.93$ mA/cm², $V_{oc}=0.65$ V, and FF= 64.7% . However, the cell with 15 nm MoO₃ exhibits a rather low PCE of 0.11% ($J_{sc}=2.13$ mA/cm² and FF= 11.0%). The IPCE spectra of these inverted OSCs are shown in Fig. 2(b). We can see that the cell with 3 nm MoO₃ has the best spectral response.

Herein, besides acting as a hole transporting/extraction layer,^{9,17,18} this MoO₃ layer functions as a protection layer preventing damage to the active layer caused by the metal deposition.¹⁹ Thus, the MoO₃ layer has to be thick enough to serve this purpose. It is worth mentioning that the MoO₃ layer has a very smooth surface (the rms roughness is less than 0.8 nm for all thicknesses studied in this work). Meanwhile, due to its high energy bandgap (~ 3 eV),²⁰ MoO₃ also serves as an exciton-blocking layer to prevent the exciton from diffusing to Ag anode side and subsequent exciton quenching there,¹⁷ beneficial to a high photocurrent. Furthermore, the higher reflection by Ag anode compared to Al cathode in regular cell helps to contribute a larger J_{sc} as well.²¹

To understand the effect of MoO₃ as an optical spacer on the J_{sc} , we then simulated the optical field distribution for a single wavelength illumination (520 nm, the maximum absorption peak of P3HT:PCBM blend) in the inverted cells with different MoO₃ thicknesses.²² The simulation result is

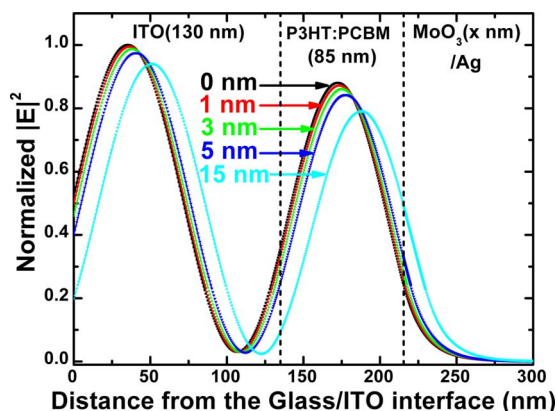


FIG. 3. (Color online) The simulated optical field distribution (for 520 nm illumination) as a function of the distance from ITO/P3HT:PCBM interface in these inverted cells. These cells have the structures of ITO/Ca(1 nm)/P3HT:PCBM(85 nm)/MoO₃(x nm)/Ag(100 nm) with $x=0, 1, 3, 5$, and 15 . The ultrathin Ca is neglected in the simulation.

shown in Fig. 3. It can be seen that the intensity maximum resides close to the center of the active layer, however, the relative optical intensity decreases with the increase of MoO₃ thickness. Particularly, for the cell with 15 nm MoO₃, the maximum peak across the active layer shifts to the anode side, showing some light leakage at the thicker MoO₃ and Ag anode side. This implies that a relatively thin MoO₃ layer is necessary for optimal performance of the cell, consistent with the experimental results.

It has to be pointed out that V_{oc} changes drastically with the thickness of MoO₃ layer [Fig. 2(a)]. Without MoO₃, V_{oc} is only 0.39 V. It can be explained by the non-Ohmic contact between P3HT:PCBM and Ag anode, i.e., the V_{oc} is correlated with the work function difference of the electrodes.²³ In this case, $V_{oc}=0.39$ V is in agreement with the work function difference of Ag (~ 4.4 eV) and ITO (~ 4.8 eV). With a 1 nm MoO₃ deposited, the P3HT:PCBM layer cannot be covered completely by MoO₃, therefore, the charge carrier loss exists at the Ag anode,²⁴ lowering the V_{oc} to 0.59 V. As the thickness of MoO₃ layer increases to 3 and 5 nm, full and uniform coverage of the active layer is established and meanwhile Ohmic contact is formed, hence the V_{oc} is determined by the difference of HOMO of P3HT and LUMO of PCBM,²⁵ and a reasonable V_{oc} of 0.65 V is obtained. However, with further increase of the MoO₃ thickness to 15 nm, the V_{oc} reduces to 0.45 V, likely caused by the voltage loss across the thick MoO₃ layer. This is different from the trend in the conventional structure where the MoO₃ thickness does not affect the V_{oc} much.²⁶

Moreover, it can be seen clearly from Fig. 2(a), that the series resistance (R_s), shunt resistance (R_{sh}), and final FF are sensitive to the MoO₃ thickness in our inverted cells. With a very thin MoO₃ layer (0 and 1 nm), the active layer may not be fully covered by MoO₃, leading to surface charge recombination at Ag anode,⁷ and hence a smaller R_{sh} (245.8 and 367.8 Ω cm² respectively). In this case, R_{sh} is the determining factor for a relatively small FF (40.3% and 41.6%, respectively). For a thicker MoO₃ layer (15 nm), a larger R_s (1121.5 Ω cm²) is introduced by MoO₃ layer itself, leading

to a poor FF of 11%, i.e., R_s is the determining factor of FF. Only with intermediate MoO₃ thickness (3 and 5 nm), the R_{sh} is large (1052.6 and 1116.1 Ω cm², respectively) and R_s is small (9.4 and 9.7 Ω cm² respectively), leading to a high FF (65.9% and 64.7%, respectively).

In conclusions, we have presented an inverted OSC using an ultrathin Ca layer as the electron-transporting layer and MoO₃ as the hole-transporting layer. ITO electrode modified by a thin Ca acts as the cathode. With an optimal MoO₃ (3 nm) as the anode buffer layer, the inverted cell has a PCE of 3.55% under simulated 100 mW/cm² illumination.

Financial support from Academic Research Fund (Grant No. RGM 44/06) of Ministry of Education, Singapore is gratefully acknowledged.

- ¹W. L. Ma, C. Y. Yang, X. Gong, K. Lee, and A. J. Heeger, *Adv. Funct. Mater.* **15**, 1617 (2005).
- ²M. Reyes-Reyes, K. Kim, and D. L. Carroll, *Appl. Phys. Lett.* **87**, 083506 (2005).
- ³L. M. Chen, Z. R. Hong, G. Li, and Y. Yang, *Adv. Mater.* **21**, 1434 (2009).
- ⁴J. Y. Kim, K. Lee, N. E. Coates, D. Moses, T. Q. Nguyen, M. Dante, and A. J. Heeger, *Science* **317**, 222 (2007).
- ⁵K. Kim, J. Liu, M. A. G. Namboothiry, and D. L. Carroll, *Appl. Phys. Lett.* **90**, 163511 (2007).
- ⁶M. Jorgensen, K. Norrman, and F. C. Krebs, *Sol. Energy Mater. Sol. Cells* **92**, 686 (2008).
- ⁷C. Tao, S. P. Ruan, X. D. Zhang, G. H. Xie, L. Shen, X. Z. Kong, W. Dong, C. X. Liu, and W. Y. Chen, *Appl. Phys. Lett.* **93**, 193307 (2008).
- ⁸S. K. Hau, H. L. Yip, H. Ma, and A. K. Y. Jen, *Appl. Phys. Lett.* **93**, 233304 (2008).
- ⁹A. K. K. Kyaw, X. W. Sun, C. Y. Jiang, G. Q. Lo, D. W. Zhao, and D. L. Kwong, *Appl. Phys. Lett.* **93**, 221107 (2008).
- ¹⁰G. Li, C. W. Chu, V. Shrotriya, J. Huang, and Y. Yang, *Appl. Phys. Lett.* **88**, 253503 (2006).
- ¹¹H. H. Liao, L. M. Chen, Z. Xu, G. Li, and Y. Yang, *Appl. Phys. Lett.* **92**, 173303 (2008).
- ¹²R. Steim, S. A. Choulis, P. Schilinsky, and C. J. Brabec, *Appl. Phys. Lett.* **92**, 093303 (2008).
- ¹³C. Tao, S. P. Ruan, G. H. Xie, X. Z. Kong, L. Shen, F. X. Meng, C. X. Liu, X. D. Zhang, W. Dong, and W. Y. Chen, *Appl. Phys. Lett.* **94**, 043311 (2009).
- ¹⁴T. Ameri, G. Dennler, C. Waldauf, P. Denk, K. Forberich, M. C. Scharber, C. J. Brabec, and K. Hingerl, *J. Appl. Phys.* **103**, 084506 (2008).
- ¹⁵C. Brabec, V. Dyakonov, J. Parisi, and N. S. Sariciftci, *Organic Photovoltaics: Concepts and Realization* (Springer, Berlin, 2003).
- ¹⁶P. W. M. Blom, M. J. M. deJong, and J. J. M. Vleggaar, *Appl. Phys. Lett.* **68**, 3308 (1996).
- ¹⁷D. W. Zhao, X. W. Sun, C. Y. Jiang, A. K. K. Kyaw, G. Q. Lo, and D. L. Kwong, *Appl. Phys. Lett.* **93**, 083305 (2008).
- ¹⁸D. W. Zhao, X. W. Sun, C. Y. Jiang, A. K. K. Kyaw, G. Q. Lo, and D. L. Kwong, *IEEE Electron Device Lett.* **30**, 490 (2009).
- ¹⁹P. Peumans, A. Yakimov, and S. R. Forrest, *J. Appl. Phys.* **93**, 3693 (2003).
- ²⁰M. Kröger, S. Hamwi, J. Meyer, T. Riedl, W. Kowalsky, and A. Kahn, *Org. Electron.* **10**, 932 (2009).
- ²¹A. K. Pandey, P. E. Shaw, I. D. W. Samuel, and J. M. Nunzi, *Appl. Phys. Lett.* **94**, 103303 (2009).
- ²²L. A. A. Pettersson, L. S. Roman, and O. Inganäs, *J. Appl. Phys.* **86**, 487 (1999).
- ²³I. D. Parker, *J. Appl. Phys.* **75**, 1656 (1994).
- ²⁴G. G. Malliaras, J. R. Salem, P. J. Brock, and J. C. Scott, *J. Appl. Phys.* **84**, 1583 (1998).
- ²⁵C. J. Brabec, A. Cravino, D. Meissner, N. S. Sariciftci, T. Fromherz, M. T. Rispens, L. Sanchez, and J. C. Hummelen, *Adv. Funct. Mater.* **11**, 374 (2001).
- ²⁶V. Shrotriya, G. Li, Y. Yao, C. W. Chu, and Y. Yang, *Appl. Phys. Lett.* **88**, 073508 (2006).